Construction and Building Materials 301 (2021) 124072

Contents lists available at ScienceDirect

Construction and Building Materials

journal homepage: www.elsevier.com/locate/conbuildmat

Assessment and prediction of cement paste flow behavior; Marsh-funnel flow time and mini-slump values

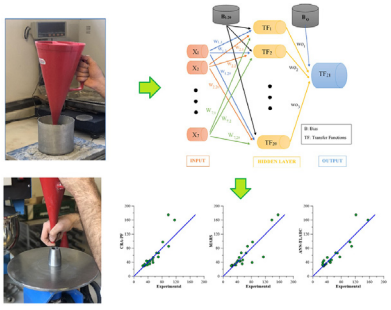
Ali Mardani-Aghabaglou [a,*], Hasan Tahsin Öztürk [b], Murat Kankal [a], Kambiz Ramyar [c]

[a] Department of Civil Engineering, Bursa Uludağ University, Nilüfer-Bursa, Turkey
[b] Department of Civil Engineering, Karadeniz Technical University, Trabzon, Turkey
[c] Department of Civil Engineering, Ege University, Bornova-Izmir, Turkey

HIGHLIGHTS

- Parameters affecting Marsh-funnel flow time and mini-slump of paste mixtures were determined.
- The study was carried out with two different approaches as experimental and modeling.
- 214 paste mixtures containing different cement/HRWR were prepared.
- Admixture content and cement fineness were found to be the most important parameters.

GRAPHICAL ABSTRACT



ARTICLE INFO

Article history:
Received 28 November 2020
Received in revised form 29 May 2021
Accepted 21 June 2021

Keywords:
Cement paste
Flowability
Neural Network
Teaching-Learning Based Artificial Bee Colony (TLABC) Algorithm

ABSTRACT

In this study, the parameters affecting Marsh-funnel flow time and mini-slump of the paste mixtures were determined through experimental and modelling studies. Marsh-funnel flow times were modelled through artificial intelligence and regression methods. A novel model was used to train the coefficients of artificial neural networks (ANN) with the Teaching-Learning Based Artificial Bee Colony (TLABC) Algorithm. Accuracy of this method was investigated through ANN-Back Propagation, ANN-Teaching Learning Based Optimization Algorithm, ANN-Artificial Bee Colony, Multivariate Adaptive Regression Splines and Classical Regression Analysis methods. ANN-TLABC method showed the best results among the applied models. The admixture content, cement fineness, solid material content of admixture and C_3A content of cement were found to be the most important parameters affecting the flowability of the paste. However, C_2S, equivalent alkali, C_4AF and C_3S contents of the cement were observed to have no considerable effect on the Marsh-funnel flowability of paste.

© 2021 Elsevier Ltd. All rights reserved.

1. Introduction

Today, superplasticizer admixtures are the most required chemical admixture type in the ready-mixed concrete industry. The production of high-strength concrete by a considerable reduction in water demand [1], increasing the construction speed by shortening the setting time [2], and producing more workable concretes with a higher service life [3] and low cost [4] are the reasons for the high utilization rate of these admixtures.

1.1. Research background

As it is known water reducing admixtures added to the mixture may not always have a positive effect [5]. Negativities may appear in the form of rapid or slow setting [6], segregation [7], rapid slump loss [8] and increase of shrinkage [9,10]. These adverse effects are

* Corresponding author.
E-mail address: ali.mardani16@gmail.com (A. Mardani-Aghabaglou).

https://doi.org/10.1016/j.conbuildmat.2021.124072
0950-0618/© 2021 Elsevier Ltd. All rights reserved.

Nomenclature

ANN	Artificial Neural Network
BP	Back Propagation
TLABC	Teaching-Learning Based Artificial Bee Colony Algorithm
TLBO	Teaching-Learning Based Optimization Algorithm
ABC	Artificial Bee Colony Algorithm
CRA	Classical Regression Analysis
LF	Linear Regression Function
PF	Power Regression Function
EF	Exponential Regression Function
MARS	Multivariate Adaptive Regression Splines
RMSE	Root Mean Square Error
MAE	Mean Absolute Error
NS	Nash-Sutcliffe
ANN-BP	Artificial Neural Network Trained by BP
ANN-TLABC	Artificial Neural Network Trained by TLABC
SSE	sum square error
MSE	mean square error
ANN-TLBO	Artificial Neural Network Trained by TLBO
ANN-ABC	Artificial Neural Network Trained by ABC
SCC	selfcompacting concrete
FRC	fiber reinforced concrete
UPV	ultrasonic pulse velocity
AI	Artificial Intelligence
ANFIS	adaptive neuro-fuzzy inference systems
SVM	support vector machine
FL	fuzzy logic
w_i	unknown regression coefficient
x_i	Independent variables
y	dependent variable
CF	cement fineness
EAC	equivalent alkali content of cement
AC	admixture content
ASC	solid content of admixture

attributed to the cement-admixture incompatibility [11]. Some of the incompatibilities might be resulted from the cement properties while some others from admixture properties or ambient conditions [12,13]. Several studies were made to understand the causes of cement-admixture incompatibility [14,15]. The simplest and most common tests to examine cement-admixture compatibility are Marsh-funnel flow and mini-slump tests. Marsh-funnel test is based on determining the flow time of the paste through the standard Marsh funnel [16]. Obviously, the paste flow time reduces by increasing the admixture dosage. However, beyond a certain admixture dosage, there will be no considerable reduction in the flow time. Such an admixture dosage is regarded as the saturation point of the admixture for the given paste. Utilization of the admixture beyond its saturation point is disadvantageous both from economic and risk of segregation viewpoints [16].

Regression is a statistical analysis method used for demonstrating the relation between two or more variables with a causal link. One of the most preferred and well-known statistical evaluation tools used in data analysis is the linear regression model. However, many relations in natural phenomena are nonlinear. Statistical analysis methods in linear and nonlinear modellings are based on the assumption of the normal distribution for the dependent variable. Multivariate Adaptive Regression Splines (MARS) used in this study is a nonparametric regression method that makes no assumption about the underlying functional relationship between dependent and independent variables [17]. Artificial Intelligence (AI) refers to the systems or machines that mimic human intelligence to perform tasks and can recursively enhance themselves based on the information they collect. These properties of the AI enabled its utilization in modelling studies frequently. In this study, hybrid models including teaching–learning based optimization algorithm (TLBO), artificial bee colony (ABC) and artificial neural network (ANN) methods were used. Currently, the most widely used approaches for modelling the cementitious system properties are ANN, adaptive neuro-fuzzy inference systems (ANFIS), support vector machine (SVM) models and the hybrid models supported by optimization algorithms. In the modeling studies, more than one model is generally used to compare the outputs of the models. In the early days when modeling studies started to become widespread, the most widely used model was ANN. This model was applied either alone [18] or in combination with classical regression analysis (CRA) and/or fuzzy logic (FL) methods [19]. Along with ANN, studies including SVM [20] and hybrid ANN [21] models became popular in time. During the last five years different studies using heuristic regression methods such as MARS [22], M5Tree [23] and support vector regression [24] became popular.

1.2. Literature review

Some previous studies on the subject are summarized below:

Aytaç [25] investigated the effect of the portland cement composition on the plasticizer admixture performance by performing Marsh-funnel and mini-slump tests. The initial fluidity was found to be related to the C_3A/ equivalent Na_2O (N_a2O_{eq}) ratio and C_4AF content of the cement. Any increase in the C_3A/Na_2O_{eq} ratio resulted in a reduction of the flow time while the increase in the C_4AF content had an opposite effect on the flow time. It was also stated that the effects of the superplasticizer properties on the initial fluidity was insignificant compared to those of the cement properties. It was emphasized that the loss of consistency varied depending on the properties of both cement and superplasticizer. A high C_3A/Na_2O_{eq} ratio decreased the consistency loss. Nkinamubanzi and Fournier [26], stated that the admixture saturation point can be foreseen as an approximate admixture dosage to provide the best rheological properties in the cementitious systems. According to Agullo et al. [27], Marsh-funnel flow time and saturation point of the mixture decreased with increasing w/c ratio. However, it was stated that increasing the admixture dosage may not necessarily increase the flowability of the paste. The variation in mixing speed and the order of adding ingredients to the mix were reported to affect the Marsh-funnel flow time. In another study [28], the effect of the Blaine fineness of a CEM I 42.5 cement on the polynaphthalene sulfonate-based superplasticizer performance was investigated by Marsh-funnel and mini-slump tests. For the compatible cement-admixture couple, the variation of cement fineness did not affect the initial Marsh-funnel flow time or initial cement paste viscosity. However, a certain increase of Blaine fineness reduced initial viscosity of the cement paste for incompatible cements. Besides, cement fineness had no considerable effect on the yield stress. Depending on the superplasticizer dosage, the initial mini-slump value or yield stress decreased when the Blaine fineness was above 3900 or 4300 cm^2/g. When the cement fineness was lower than these values the yield stresses of

the paste mixtures were nearly the same. Jarny et al. [29] found no linear relationship between viscosity and Marsh-funnel flow time of the harsh or very solid pastes with considerably low viscosity. Nehdi [30] stated that the Marsh-funnel flow time is correlated to the plastic viscosity at high mixing speeds, but to the threshold shear stress at low mixing speeds. Similar results were also reported by Khayat and Yahia [31]. Jiang et al. [9] investigated the effect of the cement alkali content on Marsh-funnel flow time, mini-slump and flow loss of the paste mixtures. For this purpose, ordinary portland cements having 0.31 to 0.93% equivalent Na_2O contents were used. The fluidity of mixtures improved, and their time-dependent flow loss reduced when cement alkali content was between 0.4 and 0.5%. Moreover, the optimum alkali content was dependent on the admixture dosage and cement type. C_3A content of cement showed no considerable effect on the fluidity of mixtures with optimum alkali content.

There are numerous studies in the literature to predict the fresh [18,23], rheological [32] and mechanical properties [33–35] as well as dimensional stability [36] of different types of cementitious systems by using artificial intelligence.

Besides, V-Funnel [37], slump flow [38,39], J-ring [40] and L-Box [41] results of cemented systems can also be obtained with great accuracy by using numeric methods such as smoothed particle hydrodynamics (SPH).

1.3. Research motivation

Owing to the complex structure of cementitious systems and the abundance of active parameters, no definite conclusion has been drawn on the flow behavior of cementitious systems yet. Besides, as can be seen from the literature review, modeling studies on the flow behavior of cementitious systems [18,23] are quite limited.

1.4. Research objective

In this study, 9 ordinary cements with varying chemical compositions were used. 214 different paste mixtures were prepared by using 3 commercially available polycarboxylate ether-based admixtures at different dosages. Marsh-funnel flow time and mini-slump values of the mixtures were measured. The parameters affecting cement-admixture incompatibility were examined. Finally, Marsh-funnel flow time values were modeled by heuristic regression and hybrid artificial intelligence methods. For this purpose, three hybrid models (ANN-TLABC, ANN-TLBO and ANN-ABC) were developed in which ANN, TLABC, TLBO and ABC methods were used together for prediction of the Marsh-funnel flow time of paste mixtures. In the ANN-TLABC model, weights belonging to the ANN method were determined by the ABC algorithm whose properties are optimized by the TLBO method. Three different ANN methods (ANN-BP, ANN-TLBO and ANN-ABC), MARS heuristic regression method and CRA with three different equations were used for verification of this method.

2. Experimental study

2.1. Materials

In this study, 9 ordinary portland cements, being commercial products of Bolu (3), Çanakkale Akçansa (2), Istanbul Nuh (1), Izmir Çimentaş (1), Söke Batıçim (1) and İzmir Batıçim (1) cement plants were used. In addition, the clinker of these cements and the gypsum used in their production were also provided. The chemical and physical properties of the cements, clinkers and gypsums are shown in Tables 1-3, respectively.

Moreover, three polycarboxylate ether- based water reducing admixtures in accordance with the TS EN 934–2 + A1 [42] Standard were also used. Admixture properties provided by their producer company are shown in Table 4.

2.2. Mixture preparation

Considering the 0.35–0.40 W/C ratio suggested in previous study [16], the W/C ratio of the mixtures was chosen as 0.35 in the Marsh-funnel and mini-slump tests. The cement and water content were kept constant in all of the mixtures. For each cement, 90 paste mixtures were prepared using 10 different proportions of each water reducing admixture varying between 0.5 and 2.75% by cement weight in addition to the control mixture without admixture.

The cement and water amount was kept constant in all mixtures. For each cement, 90 new paste mixes were prepared using 10 different proportions of water reducing additives varying between 0.5 and 2.75 w.t. % of the cement in addition to the control mixture without water reducing additives.

2.3. Testing procedures

The Marsh-funnel and mini-slump tests were conducted in accordance with the methods proposed by Aïtcin [16] and Kantro [43], respectively. For this aim, 1.2 lt. of cement paste mixture was prepared homogeneously. The mixture was poured into the Marsh-funnel (Fig. 1-a), the lower end of which was closed with a finger. Then, by lifting the finger from the tip of the funnel, the time elapsed until the 700 ml volume was emptied was measured. The measured time was recorded as the Marsh-funnel flow time of the mixture. The mixture prepared for the Marsh-funnel experiment was used in the mini-slump test. A truncated cone-shaped funnel (Fig. 1-b) with a lower inner diameter of 38.1 mm, an upper inner diameter of 19 mm and a height of 57.2 mm was used in the mini-slump test. The mixture was poured into the mini-slump funnel. The funnel was lifted vertically slowly and a period of time (10–20 s) was allowed for the flow to be completed. Then, the flow diameters in two perpendicular directions were measured with the help of a caliper and averaged and recorded.

3. Methodology of modelling

3.1. Development of models

Since the clinker and gypsum composition of C-4 cement could not be obtained, it was not taken into consideration in the modeling study. In addition, the test results of C-7 cement-bearing mixtures showed very low agreement with those of the other mixtures resulting in the reduction of models accuracy.

For this reason, the results of mixtures containing 7 different cements and 3 polycarboxylate-based admixtures in different dosages were used in modeling. Accordingly, Marsh-funnel flow time values of 159 mixtures showing no signs of segregation were used as output parameter in the models (Table S1). The Blaine fineness, C_3A, C_3S, C_2S, C_4AF and Na_2O_{eq} contents of cements as well as the admixture dosage and solid material content of the admixtures were used as input data in the models. In the examination for the input data, the Pearson correlation coefficient between C_3S and C_2S was found to be 0.98. Thus, only C_2S content was used as the input variable since the use of both variables will not contribute to the accuracy of the model and will make the model more complex. In CRA and MARS models, 136 test results (86% by total test number) and 23 test results (14% by total test number) were used for training and testing process, respectively. In ANN models, 109

Table 1
Chemical composition and physical properties of cements.

Item	C-1	C-2	C-3	C-4	C-5	C-6	C-7	C-8	C-9	
SiO_2	19.85	18.77	18.95	18.98	19.03	21.88	19.01	18.21	18.65	
Al_2O_3	4.41	3.67	3.66	4.11	4.08	3.76	2.82	3.97	5.09	
Fe_2O_3	4.14	5.05	4.95	3.48	3.42	4.05	4.64	3.17	2.45	
CaO	61.05	64.27	63.91	65.34	64.84	62.58	64.28	64.39	63.75	
MgO	1.68	1.38	1.52	1.78	1.48	1.56	1.42	1.17	2.35	
Na_2O	0.27	0.20	0.24	0.10	0.28	0.63	0.72	0.42	0.64	
K_2O	0.50	0.62	0.41	0.58	0.63	0.63	0.74	0.7	0.9	
SO_3	3.16	3.17	2.81	2.83	3.10	2.47	3.00	2.95	2.72	
Cl^-	-	0.006	0.006	0.005	0.005	0.007	0.007	0.005	-	
free CaO	1.37	1.42	1.97	1.69	1.93	1.22	0.91	1.41	1.51	
LOI	3.3	1.40	1.64	2.01	1.37	0.70	2.53	3.3	1.77	
Total	99.73	99.96	100.06	100.09	100.16	99.49	100.08	98.99	99.83	
Specific gravity	3.14	3.16	3.16	3.15	3.14	3.15	3.2	3.11	3.11	
Blaine specific surface (cm^2/g)	4260	3820	3760	3690	3900	2810	3810	3090	3510	
Residual on 0.090 mm sieve (%)	0.2	0	0	0.2	0.2	4.9	0.2	1.3	0.4	
Residual on 0.045 mm sieve (%)	1.4	1.7	2	3.1	11.4	21.5	0.3	-	-	
Residual on 0.032 mm sieve (%)	6.6	7.2	7.9	9.5	20.7	33.6	7.3	21.4	2.7	
Setting time (hour)	Initial	02:50	02:50	03:30	02:40	02:25	02:25	02:55	02:50	02:30
	Final	05:10	05:15	05:25	04:35	03:45	03:35	04:05	04:50	04:05
Normal consistency (%)	30.2	30.8	30.4	28	28.2	24.6	28.8	27.6	27.2	

Table 2
Chemical composition of clinkers.

Item	C-1	C-2	C-3	C-5	C-6	C-7	C-8	C-9
SiO_2	21.13	21.24	21.14	21.53	21.21	20.94	20.86	20.91
Al_2O_3	5.07	4.4	4.13	4.64	4.11	4.39	5.14	6.85
Fe_2O_3	4.48	5.25	5.35	3.18	4.32	5.01	3.38	2.52
CaO	65.83	65.67	65.7	66.32	65.68	64.55	66.00	66.17
MgO	1.36	1.4	1.38	1.27	1.39	1.89	1.09	1.23
Na_2O	0.30	0.32	0.32	0.34	0.33	0.37	0.35	0.34
K_2O	0.52	0.45	0.45	0.74	0.59	0.92	0.87	1.12
SO_3	0.48	0.45	0.51	0.81	1.11	0.95	1.06	0.5
Cl^-	0.008	0.009	0.015	0.016	0.014	0.011	0.012	0.008
Free CaO	1.02	1.18	1.39	1.10	1.32	1.23	1.61	2.05
C_3S	62.83	64.03	65.73	66.15	67.10	61.99	64.21	52.5
C_2S	13.20	12.63	11.05	11.86	10.20	13.31	11.39	20.37
C_3A	5.85	2.77	1.90	6.92	3.58	3.15	7.92	13.88
C_4AF	13.63	15.98	16.27	9.68	13.13	15.23	10.27	7.67

* C-4 clinker could not be obtained.

Table 3
Chemical properties of gypsums interground with clinkers.

Item	G-1	G-2	G-3	G-5	G-6	G-7	G-8	G-9
SiO_2	3.48	3.48	3.48	7.4	7.4	0.22	1.73	0.17
Al_2O_3	0.58	0.58	0.58	1.83	1.83	0	0.19	0
Fe_2O_3	0.4	0.4	0.4	0.94	0.94	0.09	0.29	0.07
CaO	32.09	32.09	32.09	29.56	29.56	31.71	33.96	33.01
MgO	1.36	1.36	1.36	1.63	1.63	1.32	1.27	1.12
Na_2O	0.47	0.47	0.47	0.59	0.59	0,43	0.43	0.46
K_2O	0.14	0.14	0.14	0.38	0.38	0	0.06	0
SO_3	38.51	38.51	38.51	38.47	38.47	40.00	39.63	38.02
LOI	22.85	22.85	22.85	19.43	19.43	22.12	21.35	22.14

* G-4 gypsum could not be obtained.
** One type of gypsum was used in C-1, C-2 and C-3 cements, which were products of the same factory. A similar situation is valid for C-5 and C-6 cements.

Table 4
Some properties of polycarboxylate ether-based high range water reducing admixtures.

Type	Alkali content (%) (Na_2O_{eq})	Density (g/cm^3)	Solids content (%)	Chloride content (%)	pH,	Operating* range (%)
SP-1	less than 5	1.098	33.5	0.012	6.54	0.6–2.0
SP-2	less than 5	1.099	33.76	0.008	6.60	0.6–2.0
SP-3	0.31	1.075	38.56	0.009	5.68	0.6–2.0

*By weight of cement



Fig. 1. The testing view, a: Marsh-funnel test, b: mini-slump test.

(69% of the total number of experiments), 27 (17% of the total number of experiments) and 23 data (14% of the total number of experiments) were used for training, validation and testing process, respectively. In order to measure the effectiveness of the models in predicting Marsh-funnel flow times for different types of cement, the data of the C-3 mixtures were used in the validation set of ANN models. In the test set common to both approaches (regression and ANN), the values of C-2 mixtures were taken into account.

3.2. Classic regression analysis (CRA)

The CRA method was initially utilized to determine the coefficients of the equations providing the most compatible results with the experimental values of the Marsh-funnel flow time. Three regression functions i.e., linear (LF), power (PF), and exponential (EF), as shown below, were used to estimate the Marsh-funnel flow time.

$$y_{Linear} = w_0 + w_1x_1 + w_2x_2 + w_3x_3 + \ldots + w_nx_n \quad (1)$$

$$y_{Power} = w_0x_1^{w_1}x_2^{w_2}x_3^{w_3}x_4^{w_4}\ldots x_n^{b_n} \quad (2)$$

$$y_{Exponential} = w_0 + \exp(w_1 + w_2x_1 + w_3x_2 + \ldots + w_{n+1}x_n) \quad (3)$$

where, (w_i) stands for the unknown regression coefficient, (x_i) and (y) are the independent and dependent variables, respectively.

3.3. Multivariate Adaptive regression Splines (MARS)

MARS is a non-parametric regression method developed by Friedman [44]. The method assumes no functional relationship between dependent and independent variables [45]. In place of this, it applies a divide and conquer strategy to explain the relationship among the variables [46]. More details about the MARS and its implementation can be found elsewhere [47,48]. The MARS model was applied to the data set and the equations as well as the basic functions giving the lowest error were determined. The Salford Predictive Modeler 8.0 software was used for the MARS model.

3.4. Artificial neural networks (ANN)

The ANN models established in the study are feed-forward and have a three layer network architecture consisting of input, hidden and output layers. Tests were applied with the numbers of 5, 10, 15 and 20 neurons to determine the optimal number of neurons in the hidden layer. In this study, ANN trained through backpropagation method (ANN-BP) as well as the hybrid ANN models trained with ABC, TLBO and TLABC algorithms that can select different transfer functions in each neuron were used. In the ANN-BP model, tangent sigmoid function was chosen as the transfer function between all layers. The number of the maximum epoch was set to 20,000 and the sum square error (SSE) goal was selected as 1×10^{-5}.

Feed-forward ANN training of the hybrid ANN model used in this study was realized through heuristic algorithms such as ABC, TLBO and TLABC. Population size of the algorithms and maximum iteration number in hybrid ANN models was considered as 100 and 10,000 times by the design variable, respectively. Design variable was searched in between the lower and upper limit (-5, 5). On the other hand, the limits of the design variables representing transfer function in each neuron were considered as separately valued as (1, 4) with an increase due to the use of four different transfer functions. 10 independent runs were carried out for each heuristic algorithm.

The ABC algorithm is inspired by the real nectar exploration behaviors of the bees. In the algorithm, the problem solutions resemble the nectar sources the bees are trying to reach, and the amount of the nectar in these sources determines the suitability of the solution in question. The bees in charge are sent to the nectar resources and the bee whose nectar source is depleted tries to discover new nectar resources in the search space, considering that it has turned into a scout bee. With this basic principle, the algorithm tries to reach the source with maximum nectar amount and tries to find the most appropriate solution that gives the minimum or maximum function value according to the aim of the problem. The detailed information about this algorithm is available in the literature [49,50].

The TLBO, which is a heuristic algorithm, was developed inspiring from the teacher's influence on students in the classroom. Problem solutions in this algorithm were represented by the teacher and the students while the best solution was considered as the teacher. There are two stages in this algorithm named as teacher and student. Training of the students by the teacher, in other words, the urge of enabling students to reach the teacher's level of information was proposed in the first stage. In the second stage, the interactions of the students with each other were taken into account. A student with a higher level of knowledge can affect a student with a lower level of knowledge by increasing his/her level. The detailed information about this algorithm is also available in the literature [51,52].

TLABC algorithm was formed with the hybridization of the ABC algorithm with the TLBO in order to cover the gaps in the exploitation strategy [53]. There are three hybrid phases in this algorithm

as teaching-based employer bee phase, learning-based onlooker bee phase and generalized opponent scout bee phase. The detailed information about this algorithm is available elsewhere [53].

In addition to the optimization of the weights during training process in the transfer function determination approach of the hybrid models, the function type of each neuron is also adopted to the problem. A distinct transfer function can be chosen for each neuron. Selection process is conducted among the transfer functions such as purelin, tangent sigmoid, logarithmic sigmoid and Elliot symmetric sigmoid. Along with the optimized weights, transfer function type in the neurons was added into the optimization process as a design variable. Minimization of the mean square error (MSE) was used as an objective function in the training. The performance of the ANN network was evaluated with root mean square error (RMSE), mean absolute error (MAE) and Nash-Sutcliffe (NS) as follows:

$$RMSE = \left[\frac{1}{n}\sum_{i=1}^{n}(E_i - P_i)^2\right]^{1/2} \quad (4)$$

$$MAE = \frac{1}{n}\sum_{i=1}^{n}|(E_i - P_i)| \quad (5)$$

$$NS = 1 - \frac{\sum_{i=1}^{n}(E_i - P_i)^2}{\sum_{i=1}^{n}(E_i - \overline{E})^2} \quad (6)$$

where E_i stands for the experimental Marsh-funnel flow time, $\overline{E}$ is the mean of these values, P_i is the value obtained from the model and n is the number of data observations. NS varies between $-\infty$ and 1. NS = 1 can be interpreted as the method is physical and excellent. Moriasi et al. [54] determined a range designating the sufficiency level of the model performance for NS statistics. A NS between 0.75 and 1 indicates that the model is very good, between 0.65 and 0.75 indicates that the model is good. If NS is between 0.50 and 0.65, the model is sufficient, and less than 0.50 indicates that the model is insufficient.

3.5. Methodology of training ANN with heuristic algorithms

The ANN training process starts with the general settings related to the network. At this stage, the input and output data for the experimental study, the number of neurons used in the hidden layer in the network, population size that the heuristic algorithm will use while optimizing the network, and the number of maximum objective function evaluation, which is the stopping criterion of the optimization process, were defined. The input data were normalized between 0.1 and 0.9 values and the data were divided into training, validation, and test data sets. Data set rates can be adjusted through the software we have prepared. However, at this stage, the algorithm (ABC, TLBO, or TLABC) to be used was selected.

In the second step, similar initial operations were done for all heuristic algorithms. Based on the information entered in the previous stage, the network architecture was created and the number of design variables that need to be optimized was calculated. Optimized design variables were weights, biases, and transfer function types. The most important feature of the methodology is that it can choose the optimum type of transfer function in each neuron. The initial population was randomly generated in this process and the objective function values of the individuals in this population were calculated. Estimated outputs were calculated according to the design variables selected during the calculation process of the objective function. Since these outputs were calculated for normalized values, they were denormalized. The amount of error was calculated by comparing with the actual values. The purpose of the algorithms was to minimize the MSE value of the training data set.

In the third step, the calculated objective function values were used by the operators of the algorithms. Algorithm operators try to improve individuals in the population based on their own strategies. In other words, they try to create a lower error-producing network. After each operator trial, the objective function evaluation process was repeated, ensuring the communication between ANN and the heuristic algorithm.

In the last stage, it was checked whether the algorithm had reached the maximum number of objective function evaluation. If not, the algorithm operators were repeated. When the stop criterion was met, the algorithm reported the optimum network achieved. The flow chart summarizing the whole process is given in Fig. 2.

4. Results and discussion

4.1. Evaluation of the experimental results

Marsh-funnel flow times of the paste mixtures are shown in Table 5. Moreover, the flow time curves of the mixtures containing various amounts of each admixture are also shown in Figs. 3-11. As expected, Marsh-funnel flow times of the mixtures decreased while the water reducing admixture content increased. However, beyond a certain admixture content no considerable change was observed in the flow time of the mixtures. This admixture dosage is defined as the saturation point of the admixture.

According to the producer company, C-1, C-2 and C-3 cements were manufactured from the same raw materials in different proportions. In addition, the same gypsum grinded with the clinker was used during the manufacturing of these cements. Thus, the compound composition of these cements, including their C_3A content, is quite different. The C_3A contents of C-1, C-2 and C-3 cements are 5.85, 2.77 and 1.90%, respectively. Cement C_3A content is a significant factor affecting the cement–water reducing admixture compatibility [14]. According to the results, irrespective of the admixture type, in C-1, C-2 and C-3 cements-bearing mixtures the admixture saturation point was found to be 1.25%. However, when Marsh-funnel flow times at admixture saturation point were considered, flow times of the mixtures reduced with the reduction of cement C_3A content. Flow time of the mixture with 5.85% C_3A content cement was observed to be nearly 30% and 45% more than those with 2.77 and 1.90% C_3A cements, respectively. According to the literature, high C_3A compound in the cement is undesirable in terms of the fresh state and rheological properties of the cementitious system [14,20,55]. The needle-like ettringite crystals formed as a result of the C_3A hydration consume a great amount of the mixing water. Thus, workability of the cementitious system reduces [5,14,33]. More calcium sulfoaluminate hydrate products are formed when the cement C_3A content is high. According to Prince et. al. [56], in the early stages of cement hydration, C_3A compound releases $Al(OH)_4^-$ ions, which allow the formation of ettringite crystals. Hence, the ettringite crystals begin to form in the system. According to the same researchers, a considerable amount of admixture is tied up in the ettringite crystals or is adsorbed on their surface. Thus, less admixture remains for dispersion of unhydrated cement particles. As a result, fresh properties of the cementitious system are negatively affected.

Irrespective of the admixture type, the saturation point was observed to be 1.5% in C-4 cement-bearing pastes. Generally finer cements with higher specific surface area are expected to have a higher admixture demand for a certain flow. However, in spite of having a higher fineness, C-3 cement was superior to C-4 cement in terms of the admixture saturation point and paste flowability.

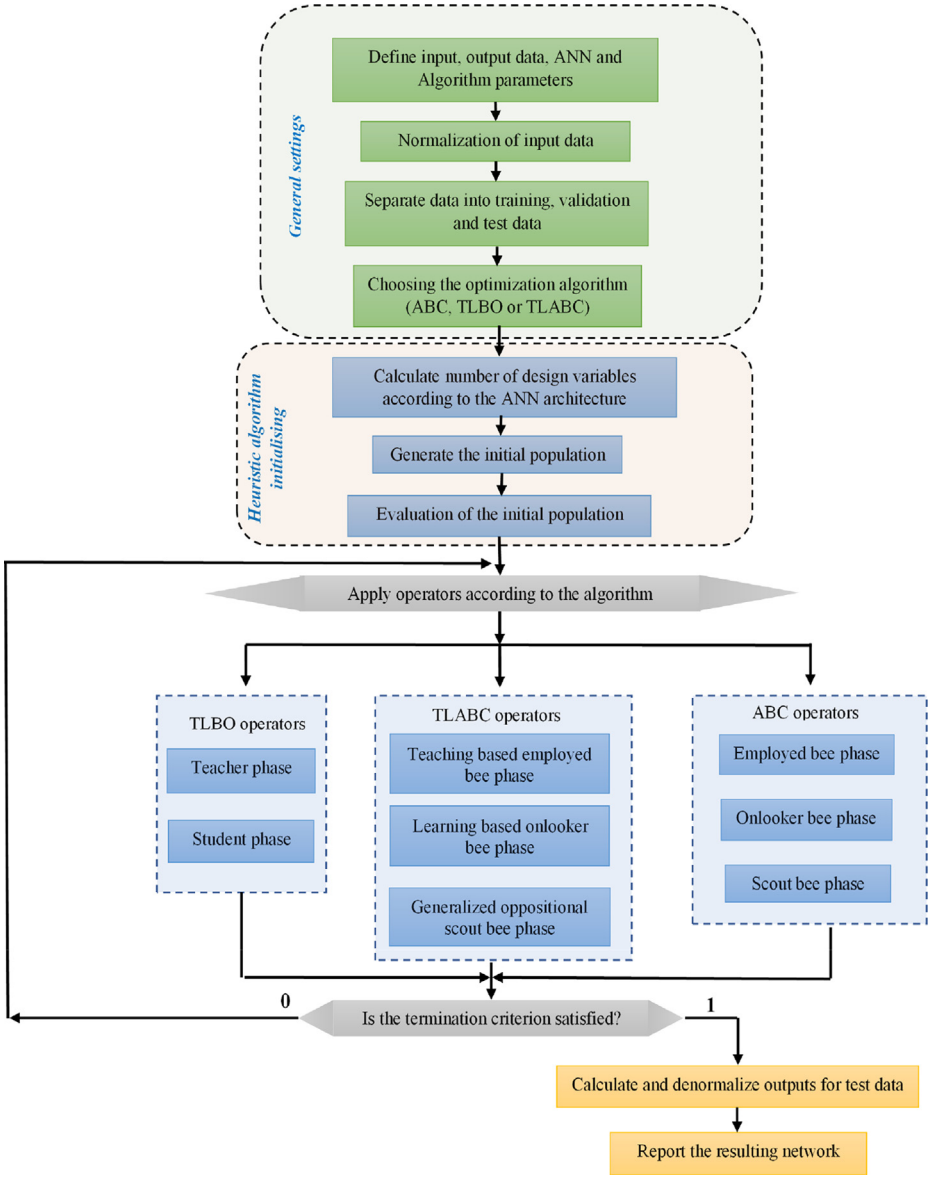


Fig. 2. Flow chart of training ANN with heuristic algorithms.

Therefore, the cement fineness is not the only parameter affecting the flow performance of the paste mixtures. The superior performance of C-3 cement in terms of paste flowability seems to be arisen from its lower C_3A content.

C-5 and C-6 cements were supplied from the same factory. The admixture saturation points in the pastes containing these cements was 1.5% (corresponding to a flow time of around 35 s) and 1.25% (corresponding to a flow time of about 30 s), respectively. As it can be seen from Table 1, the Blaine finenesses of C-5 and C-6 cements are 3900 cm^2/g and 2810 cm^2/g, respectively. Moreover, C-5 cement includes 50% more C_3A than C-6. The higher performance of C-6 cement in terms of paste flowability was attributed to its lower C_3A content and lower fineness than those of C-5 cement.

Irrespective of admixture type, in paste mixtures containing C-7 cement, the admixture saturation point was determined when the admixture/cement ratio was 1%. It can be understood from Table 2 that the C_3A contents of C-7 and C-6 cements are 3.15% and 3.58%, respectively. Although both cements contain very close C_3A content, C-6 mixture showed better behavior than C-7 in terms of the flow performance. It should also be noted that C-7 cement was 1.35 times finer than the C-6 cement (Table 1).

Figs. 10 and 11 reveal that the admixture saturation point was 1% in C-8 and 0.75% in C-9 mixtures, respectively. Even though C_3A content of the C-9 cement was 3 times higher than that of the C-1, it showed better performance in terms of paste flow performance. Besides, the Blaine fineness of C-9 cement (3510 cm^2/g) is somewhat lower than that of C-1 cement (4260 cm^2/g). Results demonstrated that the cement fineness and C_3A content are two main parameters affecting the flow performance of paste mixtures. Nevertheless, since these cements were produced from different raw materials and include different amounts and types of gypsum, it was impossible to determine the exact effect of each parameter on the flow of paste mixture. Therefore, a statistical modelling method was conducted.

Mini-slump test results and temperatures of the 214 paste mixtures prepared with 27 different cement-admixture couples are shown in Tables 6 and 7, respectively. The Mini-slump values of all mixtures increased with the increase of admixture content up to a certain level. However, increasing the admixture content

Table 5
Marsh-funnel flow time values of paste mixtures (s).

Admixture-Mixture		Admixture/cement ratio (%)									
		0.5	0.75	1	1.25	1.5	1.75	2	2.25	2.5	2.75
SP-1	C-1	190	109.4	60	46.2	44.52	41.78	41.43	40.25	40.47	–*
	C-2	175	55.3	39.5	35.4	32.5	31.8	30.1	29.4	29.8	–
	C-3	90	48.3	39.2	32.31	30.3	28.8	28.2	26.4	29.1	–
	C-4	135	110	58.53	41.5	34.82	32.28	31.57	30.34	29.38	28.72
	C-5	68	59.63	46.25	40.72	34.25	31	28.78	28.00	26.41	25.82
	C-6	51	39.5	35	30.28	26.19	24.93	23.1	23.41	–	–
	C-7	280	175	37.53	34.22	34.1	33.41	35.03	–	–	–
	C-8	119	91.5	52	46.28	37.06	40	–	–	–	–
	C-9	55	29.97	28.56	29.91	–	–	–	–	–	–
SP-2	C-1	94.23	83.31	60	44.28	42	35	34	32.00	32.2	–
	C-2	85.3	66.88	53.5	45	39.84	32	34.4	–	–	–
	C-3	66.32	59.56	45	38	36	33	32.57	30.63	30.59	29.34
	C-4	95	82.5	42	32.56	30.53	28.4	27.41	27.13	26.66	26.56
	C-5	49	44.5	45.06	39.75	35	32.25	30.03	29.38	27.09	26.13
	C-6	38.56	34.62	30.75	27.56	24.91	23.87	21.16	21.50	–	–
	C-7	145	115.2	44.97	36	32.66	32.03	32	34.47	–	–
	C-8	88	59.34	38.13	33.59	30	30.22	–	–	–	–
	C-9	73	44.78	43.52	30.5	28.35	27.56	–	–	–	–
SP-3	C-1	160	86.25	67.1	52.7	46.03	44.19	43.06	43.65	–	–
	C-2	160	97.69	66.43	46.53	43.1	42.65	44.04	–	–	–
	C-3	160	81.75	63.73	53.97	47	45.2	43.59	42.88	41.97	42.9
	C-4	91	75.31	40	32.19	30.1	29.94	29.4	29.25	28.5	29.97
	C-5	60	45.68	39.91	36.47	34.22	32.94	32.47	31.43	31.35	31.47
	C-6	49	36.47	31.3	28	26.91	26.66	26.19	24.79	25.4	–
	C-7	–	220	60	58	57.4	58	–	–	–	–
	C-8	110	85	53.46	44.72	45	–	–	–	–	–
	C-9	69	44.59	37.65	38.03	–	–	–	–	–	–

*No measurement could be taken due to segregation.

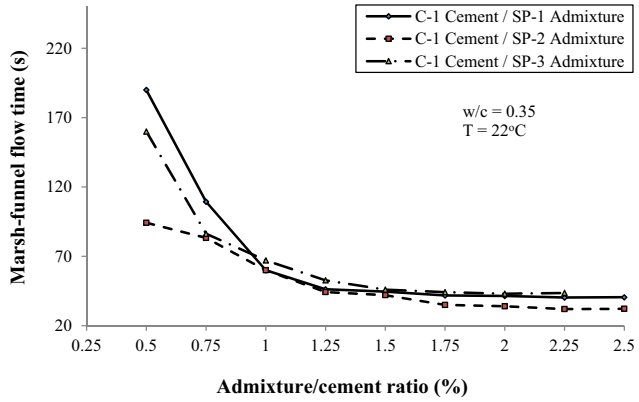


Fig. 3. Marsh-funnel flow times of C-1 pastes containing various amounts of admixtures.

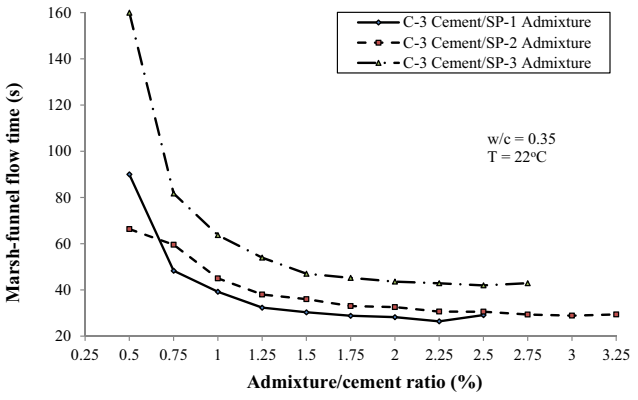


Fig. 5. Marsh-funnel flow times of C-3 pastes containing various amounts of admixture.

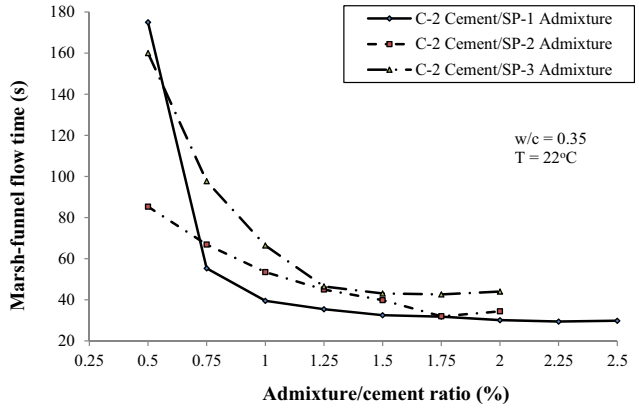


Fig. 4. Marsh-funnel flow times of C-2 pastes containing various amounts of admixtures.

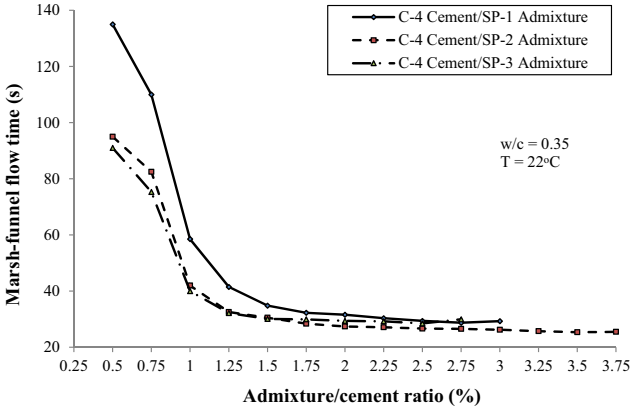


Fig. 6. Marsh-funnel flow times of C-4 pastes containing various amounts of admixtures.

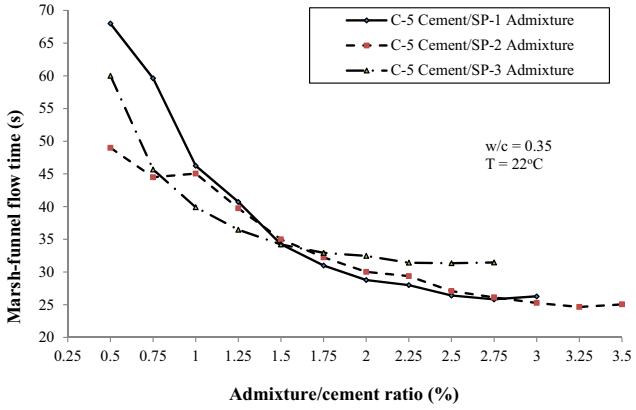


Fig. 7. Marsh-funnel flow times of C-5 pastes containing various amounts of admixtures.

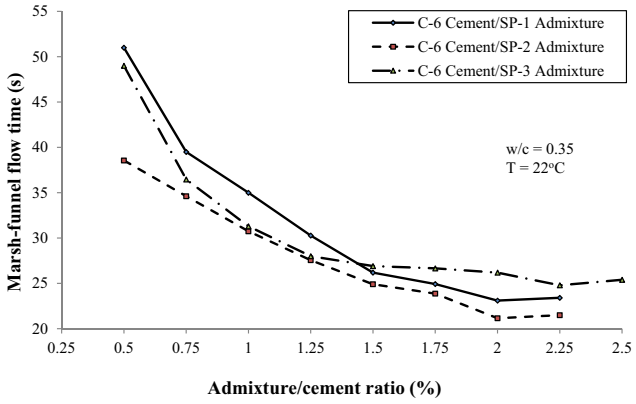


Fig. 8. Marsh-funnel flow times of C-6 pasts containing various amounts of admixture.

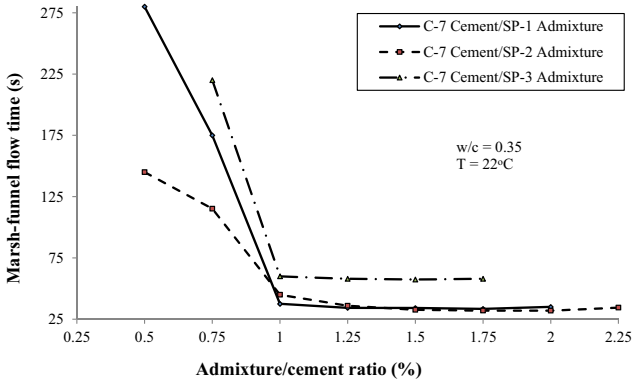


Fig. 9. Marsh-funnel flow times of C-7 pastes containing various amounts of admixtures.

beyond this level had not a significant effect on the slump of paste; even in some cases it resulted in the extreme cohesiveness and segregation of the paste. Table 7 shows that there was not a considerable change in the temperature of pastes with the alteration of admixture type and ratio.

4.2. Evaluation of the modelling results

4.2.1. Regression analysis results

In this section, three different regression functions of CRA method as well as equations and the error values of the MARS

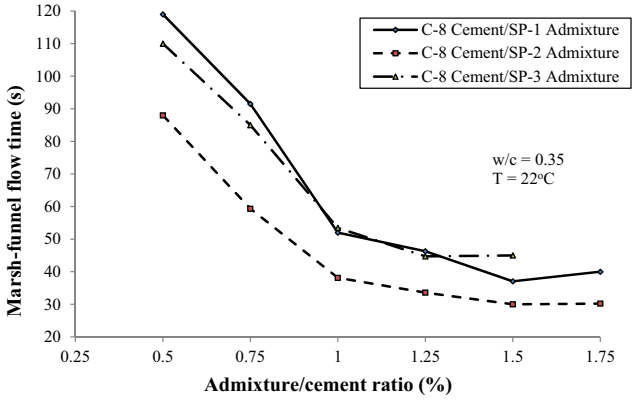


Fig. 10. Marsh-funnel flow times of C-8 pastes containing various amounts of admixtures.

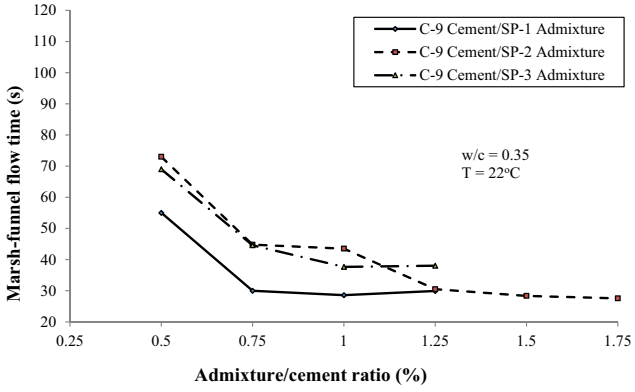


Fig. 11. Marsh-funnel flow times of C-9 pastes containing various amounts of admixtures.

model are given. The regression equations and related parameters of the linear and exponential functions used in the CRA method are shown in Table 8. Fundamental functions for the MARS model and the most convenient equation found through these functions is shown in Table 9. In these Tables, (x_1), (x_2), (x_3), (x_4), (x_5), (x_6), (x_7) and (y) stand for cement fineness (CF), C_3A, C_2S, C_4AF, equivalent alkali content of cement (EAC), admixture content (AC), solid content of admixture (ASC) and Marsh-funnel flow time of the paste, respectively.

The error values of all regression equations are calculated separately for training and testing set (Table 10). According to the error values, MARS method showed better results than CRA equations. The performance of MARS is noticeably better than CRA functions, especially in the training set. While the NS value was 0.85 in the best CRA function (EF), this value increased to 0.977 in the MARS model. The MARS model was not able to show the same performance in the test set. Although the MARS model gave much better results than LF and EF, it was only able to provide an improvement of 0.045 in NS compared to PF. Among the CRA equations, on the other hand, EF showed better results for training while PF for testing set.

4.2.2. ANN modelling results

RMSE, MAE and NS values were used to compare the performances of the BP, ABC, TLBO and TLABC algorithms used to determine the best ANN representing the test results. 10 independent runs with particular numbers of neurons were realized to determine the performances of the heuristic algorithms. The statistical data obtained for RMSE, MAE and NS values are shown in Table 11.

Table 6
Mini-slump values of paste mixtures (mm).

Admixture-Mixture	Admixture/cement ratio (%)										
	0.5	0.75	1	1.25	1.5	1.75	2	2.25	2.5	2.75	
SP-1	C-1	140	150	170	175	180	180	175	180	–*	–
	C-2	150	170	175	180	180	180	180	180	–	–
	C-3	150	175	175	180	180	185	185	190	–	–
	C-4	140	150	150	160	160	170	170	180	180	180
	C-5	140	150	150	160	160	170	170	170	170	170
	C-6	140	160	160	170	170	170	170	170	–	–
	C-7	115	120	170	180	190	180	180	–	–	–
	C-8	140	160	170	180	180	170	–	–	–	–
	C-9	150	175	175	175	–	–	–	–	–	–
SP-2	C-1	140	155	165	175	175	180	175	175	175	–
	C-2	150	170	175	175	180	180	180	180	180	180
	C-3	150	170	170	170	175	175	175	–	–	–
	C-4	140	145	170	170	170	180	180	180	180	180
	C-5	145	160	160	170	170	170	170	170	170	170
	C-6	150	160	160	170	170	175	175	180	–	–
	C-7	110	115	180	190	190	190	190	190	–	–
	C-8	130	160	160	170	170	170	–	–	–	–
	C-9	140	150	165	175	175	175	–	–	–	–
SP-3	C-1	140	170	190	190	190	195	195	195	–	–
	C-2	140	170	170	170	170	175	175	180	180	180
	C-3	145	160	170	170	170	170	170	–	–	–
	C-4	135	160	160	170	170	170	170	170	170	170
	C-5	140	160	160	170	170	175	175	175	175	175
	C-6	140	165	165	165	170	170	165	160	–	–
	C-7	105	110	170	180	185	185	–	–	–	–
	C-8	140	160	165	175	180	–	–	–	–	–
	C-9	140	160	160	160	–	–	–	–	–	–

* No measurement could be taken due to segregation.

Table 7
Temperature of paste mixtures (°C).

Admixture-Mixture	Admixture/cement ratio (%)										
	0.5	0.75	1	1.25	1.5	1.75	2	2.25	2.5	2.75	
SP-1	C-1	28.1	27.7	27.6	26.9	27.8	27	27.5	27.6	27.8	-*
	C-2	27.1	27.3	26.7	26.5	26.5	26.9	26.7	26.1	26.0	–
	C-3	28.5	27.9	26.6	26.3	26.3	26.8	26.5	26.1	26.1	–
	C-4	24.1	24.3	25	25.3	25.3	25.2	25.4	25.4	25.7	25.5
	C-5	25	25.1	25.9	26.2	26.2	26.1	26.4	26	26.1	25.9
	C-6	24.5	24	24.7	25	25.2	25.2	25.1	25	–	–
	C-7	31.5	31	30.4	30.5	30	31	31.5	–	–	–
	C-8	21	21	20.9	21.5	21.5	21.1	–	–	–	–
	C-9	23.5	23.8	24.5	25	–	–	–	–	–	–
SP-2	C-1	27.5	27.2	27.5	26.5	26.2	26	25.7	26.5	27	–
	C-2	25.5	25.2	25.9	25.9	25.7	25.5	25.4	–	–	–
	C-3	26.2	26.5	27.3	28	27.1	26.8	26.4	–	–	–
	C-4	26.5	26	26.8	26.6	26.3	26.4	26	25.9	25.6	25.3
	C-5	25.9	25.6	25.4	25.7	26	26.1	26.1	26.2	26.2	26.2
	C-6	24.7	25	24.9	25.2	25.1	25.5	25.4	25.4	–	–
	C-7	30.1	30.3	29.8	29.5	29.3	29	28.8	–	–	–
	C-8	22.2	22.5	22.5	22.2	23.1	23.3	–	–	–	–
	C-9	25.4	25.5	24.3	24.6	25.2	25.1	–	–	–	–
SP-3	C-1	27	26.7	27.4	26.8	25.9	25.3	24.9	24.5	–	–
	C-2	27.3	27.1	26.7	26.9	26.6	26.2	26.1	25.8	25.6	25.4
	C-3	28	27.7	30.2	28.5	27.2	27.3	27.2	–	–	–
	C-4	26.6	27.2	27.1	27.6	27.5	27.5	27.5	27.4	27.4	27.4
	C-5	26.3	26.8	25.9	25.9	27.3	27.3	27	27.1	27.8	27.8
	C-6	26.4	26.8	26.9	27.1	26.8	27.1	27.3	27.1	27.5	–
	C-7	30.8	30.5	29.2	28.9	28.7	28.4	–	–	–	–
	C-8	23.8	23.5	23.3	23.5	23.8	–	–	–	–	–
	C-9	24.6	24.5	25.4	24.7	–	–	–	–	–	–

* No measurement could be taken due to segregation.

On the other hand, RMSE, MAE and NS values of the training, validation and testing data for best solutions determined in independent runs performed with heuristic algorithms are shown in Table 12. The best solution for all data was the one where the minimum error was observed.

According to Table 11, in the case of 5 neurons in the hidden layer, the best values of RMSE, MAE and NS obtained in the training set were obtained by TLABC algorithm as 8.560, 4.979, and 0.895, respectively. In the case of 10 neurons in the hidden layer, the best values of RMSE, MAE and NS obtained in the training set were

Table 8
Coefficients obtained from CRA.

Models	Coefficients								
	w_0	w_1	w_2	w_3	w_4	w_5	w_6	w_7	w_8
LF	−131.312993	0.016433	12.954411	−8.512472	10.624249	−1.24642	27.052374	1.577429	–
PF	3,854,662.568765	−3.005224	0.985387	1.085042	1.63508	−2.323878	−0.848672	1.188982	–
EF	29.748596	−1.6727	−0.00022	0.76906	−0.313498	0.589894	−3.001763	−2.412802	0.055568

$y_{LF} = w_0 + w_1X_1 + w_2X_2 + w_3X_3 + w_4X_4 + w_5X_5 + w_6X_6 + w_7X_7$

$y_{PF} = w_0{X_1}^{w_1}{X_2}^{w_2}{X_3}^{w_3}{X_4}^{w_4}{X_5}^{w_5}{X_6}^{w_6}{X_7}^{w_7}$

$y_{EF} = w_0 + \exp(w_1 + w_2X_1 + w_3X_2 + w_4X_3 + w_5X_4 + w_6X_5 + w_7X_6 + w_8X_7)$

Table 9
Basic functions and equation obtained from MARS for Marsh funnel flow times.

Basic functions
BF1 = C(AC|+1,0.875,1,1.25)
BF2 = C(AC|-1,0.875,1,1.25) * C(CF|+1,3830,3900,4080)
BF3 = C(AC|-1,0.875,1,1.25) * C(CF|-1,3830,3900,4080)
BF4 = BF3 * C(C_2S|-1,10.625,11.05,15.71)
BF5 = C(EAC|+1,0.60216,0.69454,0.96337)
BF6 = C(ASC|-1,33.63,33.76,36.16) * C(C_3A|-1,4.715,5.85,6.885)
BF7 = C(C_3A |+1,6.885,7.92,10.9)
BF8 = BF1 * C(ASC|+1,33.63,33.76,36.16)
BF9 = BF1 * C(ASC|-1,33.63,33.76,36.16)
BF10 = C(C_3A|-1,6.885,7.92,10.9) * C(AC|+1,0.625,0.75,0.875)
BF11 = C(AC|-1,1.25,1.5,1.75) * C(ASC|+1,33.63,33.76,36.16)
BF12 = C(AC|-1,1.25,1.5,1.75) * C(ASC|-1,33.63,33.76,36.16)
BF13 = BF12 * C(CF|-1,3425,3760,3830)
BF14 = BF13 * C(C_3A|+1,6.885,7.92,10.9)
BF15 = BF13 * C(C_3A|-1,6.885,7.92,10.9)
BF16 = C(C_3A|-1,6.885,7.92,10.9) * max(0, ASC-33.5)
BF17 = BF16 * C(AC|+1,1.75,2,2.25)
BF18 = BF16 * C(AC|-1,1.75,2,2.25)
BF19 = BF10 * max(0,38.56 -ASC)
BF20 = BF11 * C(CF|-1,2950,3090,3425)
BF21 = BF9 * C(CF|+1,3830,3900,4080)
BF22 = C(C_3A|-1,6.885,7.92,10.9) * C(AC|-1,0.625,0.75,0.875) * C(CF|+1,3830,3900,4080)
BF23 = C(AC|-1,1.25,1.5,1.75) * C(ASC|+1,33.63,33.76,36.16) * C(CF|+1,2950,3090,3425) * C(C_3A|+1,4.715,5.85,6.885)
BF24 = BF16 * C(C_4AF|-1,10.65,13.63,14.95)
BF25 = C(AC|-1,0.625,0.75,0.875)
BF26 = BF25 * C(CF|+1,3425,3760,3830)
BF27 = BF25 * C(CF|-1,3425,3760,3830)
BF28 = BF12 * C(C_3A|+1,2.74,3.58,4.715)
BF29 = BF12 * C(C_3A |-1,2.74,3.58,4.715)
BF30 = C(AC|+1,0.625,0.75,0.875) * C(ASC|-1,33.63,33.76,36.16) * C(CF|+1,3425,3760,3830)
Marsh funnel flow time = 43.154–10.434*BF1 + 0.24428*BF2 + 0.10052*BF3 −0.097567*BF4 −30.712*BF5 −17.021*BF6 + 1.5764*BF7 + 3.1235*BF8 + 48.634*BF9 + 26.786*BF10 + 7.1414*BF11 + 680.3*BF12 + 0.17085*BF13 + 0.71863*BF14 −0.15209*BF15 −6.6924*BF16 −5.6397*BF17 + 5.5315*BF18 −5.2607*BF19 −0.026582*BF20 + 0.67891*BF21 + 0.55772*BF22 −0.0024337*BF23 −0.67584*BF24 + 107.46*BF25 −0.87503*BF26 −0.1537*BF27 −179.36*BF28 −329.58*BF29 −0.42357*BF30

Table 10
RMSE, MAE and NS values of CRA and MARS in training (training + validation for ANN) and testing set.

Data Set	Training (Training + Validation for ANN)				Testing			
Model	LF	PF	EF	MARS	LF	PF	EF	MARS
RMSE	17.59	11.60	10.31	4.02	29.97	19.85	25.59	18.12
MAE	11.63	8.15	6.61	2.83	15.48	10.37	12.86	11.75
NS	0.563	0.810	0.850	0.977	0.387	0.731	0.553	0.776

obtained with the TLABC algorithm as 7.598, 4.388, and 0.917, respectively. In the case of 15 neurons in the hidden layer, the best values of RMSE, MAE and NS obtained in the training set were obtained with the TLABC algorithm as 6.656, 3.733, and 0.937, respectively. In the case of 20 neurons in the hidden layer, the best values of RMSE, MAE and NS obtained in the training set were obtained by TLBO algorithm as 6.309, 3.480, and 0.943, respectively. However, while deciding on the predictive performance of the network, the error of the test data is checked. As such, the low error value of the TLBO algorithm for 20 neurons does not mean that the network's prediction performance is good. When the standard deviation of the independent run is examined, it is understood that the TLABC algorithm generally has a lower standard deviation than the others. This shows that the TLABC algorithm gives more consistent results than others.

In addition, Friedman rank test was performed to compare the performances of the algorithms. Table 12 shows Friedman rank test results for the best solutions obtained for all runs. According to this table, the algorithms are ranked as TLABC, TLBO and ABC, respectively, according to their performance.

When the RMSE values of the test set in Table 13 are examined, it is seen that as the number of neurons in the hidden layer

Table 11
RMSE, MAE, and NS values for training dataset obtained from ten independent runs.

Number of Neuron	Status	ABC			TLBO			TLABC		
		RMSE	MAE	NS	RMSE	MAE	NS	RMSE	MAE	NS
5	Best	9.380	5.385	0.874	9.046	5.329	0.883	8.560	4.979	0.895
	Worst	10.267	6.072	0.849	9.664	5.747	0.866	10.133	5.730	0.853
	Mean	9.915	5.898	0.859	9.344	5.621	0.875	9.109	5.346	0.881
	Std.Var.	0.394	0.258	0.011	0.200	0.153	0.005	0.563	0.238	0.015
10	Best	8.329	5.501	0.901	7.641	4.111	0.917	7.598	4.388	0.917
	Worst	9.900	6.850	0.860	9.169	5.343	0.880	8.655	4.901	0.893
	Mean	9.345	6.061	0.875	8.268	4.675	0.902	8.162	4.607	0.905
	Std.Var.	0.568	0.440	0.015	0.569	0.395	0.014	0.393	0.201	0.009
15	Best	8.755	5.419	0.890	7.014	4.181	0.930	6.656	3.733	0.937
	Worst	9.822	6.483	0.862	8.177	4.665	0.904	7.984	4.341	0.909
	Mean	9.452	5.982	0.872	7.761	4.374	0.914	7.269	3.980	0.924
	Std.Var.	0.391	0.380	0.010	0.407	0.159	0.009	0.426	0.225	0.009
20	Best	8.512	5.488	0.896	6.309	3.480	0.943	6.695	3.516	0.936
	Worst	10.017	6.270	0.857	7.715	4.236	0.915	7.097	3.770	0.928
	Mean	9.374	6.050	0.874	7.099	3.862	0.928	6.904	3.653	0.932
	Std.Var.	0.489	0.284	0.013	0.459	0.241	0.009	0.159	0.102	0.003

Table 12
Friedman rank test results for the best solutions obtained for all runs.

Algorithms	Normalized Friedman value	Rank
ABC	2.9500	3
TLBO	1.7000	2
TLABC	1.3500	1

increases from 5 to 20, the errors generally decrease and the NS values increase accordingly. According to the NS values, all the models were classified as very good. Table 13 also demonstrates that TLABC algorithm solutions are better than those of the others except for the situation when there are 5 neurons in the hidden layer. All these findings show that the model with the highest predictive performance among the hybrid ANNs is TLABC-ANN. The network architecture in which the optimized variables are named is given in Fig. 12. The optimum weights, biases and transfer functions selected by the TLABC algorithm for the optimum network with 20 neurons in its hidden layer are presented in Table 14.

4.2.3. Comparing modelling results

The testing data set was used to compare the model performances since the data set was divided into three in ANN models and two in the other models. Table 15 demonstrates the RMSE, MAE and NS values for testing data set in order to evaluate the Marsh-funnel flow time estimation capabilities of the CRA, MARS and ANN models. Results indicating the lowest error values for Marsh-funnel flow time (as well as the highest NS value) were marked in bold.

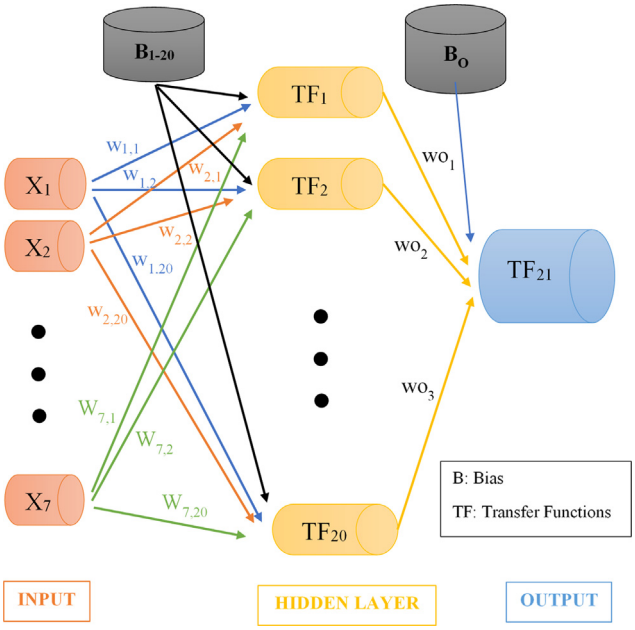


Fig. 12. ANN architecture.

When the error and NS values obtained from the models are examined, it is seen that the best performance among the methods is shown by the ANN-TLABC model. However, for this problem, it is

Table 13
RMSE, MAE, and NS values in training, validation and test dataset for the best solution in independent runs.

Number of Neuron	Models	Training Dataset			Validation Dataset			Testing Dataset		
		RMSE	MAE	NS	RMSE	MAE	NS	RMSE	MAE	NS
5	ANN-ABC	9.49	5.39	0.871	9.57	6.75	0.875	15.69	9.70	0.832
	ANN-TLBO	9.28	5.62	0.877	6.41	4.76	0.944	17.08	9.38	0.801
	ANN-TLABC	9.15	5.32	0.880	7.52	5.09	0.923	17.52	9.48	0.790
10	ANN-ABC	9.21	6.85	0.879	6.22	4.47	0.947	16.82	11.11	0.807
	ANN-TLBO	7.64	4.11	0.917	6.19	4.13	0.948	16.96	12.16	0.803
	ANN-TLABC	8.05	4.39	0.907	6.20	4.26	0.948	14.46	8.26	0.857
15	ANN-ABC	8.76	5.42	0.890	8.95	6.05	0.891	20.35	8.80	0.717
	ANN-TLBO	7.80	4.35	0.913	5.73	4.24	0.955	16.21	11.08	0.820
	ANN-TLABC	7.14	3.75	0.927	6.32	4.74	0.946	15.93	8.86	0.827
20	ANN-ABC	9.57	6.27	0.869	8.47	6.07	0.902	19.33	9.79	0.745
	ANN-TLBO	6.31	3.48	0.943	5.85	4.65	0.953	14.62	8.78	0.854
	ANN-TLABC	6.91	3.68	0.932	6.14	4.83	0.949	14.28	8.47	0.861

Table 14
Optimum weights, biases and transfer functions selected by the TLABC algorithm.

	Weights							Bias	Transfer Functions	Weights	Bias	Transfer Functions (output)
j	$W_{1,j}$	$W_{2,j}$	$W_{3,j}$	$W_{4,j}$	$W_{5,j}$	$W_{6,j}$	$W_{7,j}$	B_j	TFj	$W_{o,j}$	Bo	TF_{21}
1	1.120038	−2.51629	0.242651	−1.19378	1.263451	4.997757	−0.55263	0.922665	Tansig	−3.10635	0.196562	Logsig
2	0.022753	4.972974	4.993917	−1.37713	−0.90532	4.362569	1.929973	1.083568	Logsig	3.217397		
3	0.055511	1.836857	0.31259	0.920222	−2.26309	−4.99991	4.872516	−4.9982	Logsig	4.999381		
4	−0.81498	0.806145	1.56006	−1.11458	−0.60473	4.999056	−4.9977	−2.27713	Tansig	−0.2883		
5	−0.46386	0.70528	−1.86219	−0.93786	0.873119	4.040122	−0.8145	−2.81382	Tansig	−0.82115		
6	−1.8419	2.314239	−4.96527	1.112306	−3.40964	−1.1032	−0.07619	−2.14415	Elliotsig	−1.67899		
7	−0.40387	−4.35556	−1.14767	0.296173	−1.24587	3.780907	−4.84956	−4.8658	Tansig	−4.57578		
8	1.766463	−0.37859	1.056208	−1.09102	2.188481	−2.62897	−4.99708	1.769214	Tansig	−1.70392		
9	1.664705	1.377682	−0.15073	2.67043	1.360794	−4.99935	−0.68494	−1.18024	Logsig	−2.47707		
10	2.301109	−0.23302	−2.64214	−4.99706	1.273273	−4.9931	−0.09618	−0.91768	Elliotsig	−4.97562		
11	2.244861	4.952814	1.991109	−2.32483	1.406339	−0.40724	4.991814	1.895647	Logsig	2.535906		
12	−1.34014	−4.9358	−4.99464	1.456333	−0.26459	−4.92606	−2.91493	0.211184	Logsig	−2.826		
13	1.904689	−3.64233	−4.99836	−4.43578	−1.00624	1.016138	4.999956	4.022433	Tansig	−2.09599		
14	−3.07453	0.956814	4.548067	1.656754	−1.75967	1.368919	4.999966	0.058967	Tansig	−4.65825		
15	0.326803	0.468426	2.267338	4.939525	−1.9048	−0.31722	−0.28214	−1.70664	Tansig	0.815111		
16	−4.46074	0.212784	1.486513	0.336074	0.428164	1.481221	−0.29882	−2.11231	Logsig	−0.42539		
17	2.747777	−4.9008	−4.73443	−0.14985	0.953414	−4.99794	1.238944	0.419265	Tansig	−0.52526		
18	−2.47259	0.513492	−1.12811	0.19331	1.307961	−3.50493	−0.80143	0.062815	Tansig	1.627639		
19	0.491347	4.972669	4.695871	1.63658	0.200557	1.372823	0.151544	−1.79393	Tansig	2.263062		
20	−0.25234	1.313072	0.136076	1.814253	−1.48589	−4.99995	−1.49999	−0.62783	Logsig	4.999559		

Table 15
RMSE, MAE and NS values of CRA, MARS and ANN models in testing set.

Model	LF	PF	EF	MARS	ANN-BP	ANN-ABC	ANN-TLBO	ANN-TLABC
RMSE	29,97	19,85	25,59	18,12	15,83	15,69	14,62	14,28
MAE	15,48	10,37	12,86	11,75	8,47	9,70	8,78	8,47
NS	0,387	0,731	0,553	0,776	0,829	0,832	0,854	0,861

Table 16
Validity limits of the models.

Limit	CF (cm^2/g)	C_3A (%)	C_2S (%)	C_4AF (%)	EAC (%)	AC (%)	ASC (%)
Minimum	2810	1.90	10.20	7.67	0.51	0.5	33.50
Maximum	4260	13.88	20.37	16.27	1.23	2.5	38.56

Table 17
Relative importance of the input variables on Marsh funnel in the MARS.

Variable importance for Marsh funnel (%)		
Admixture/cement ratio	100						

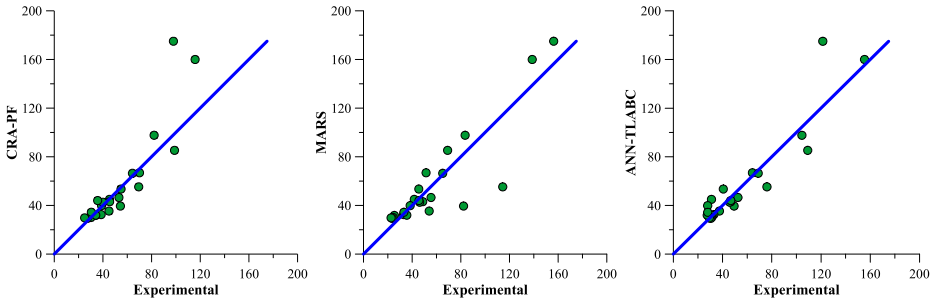


Fig. 13. Scatter plots of the experimental results with the estimated ones by the CRA-PF, MARS and ANN-TLABC for testing datasets.

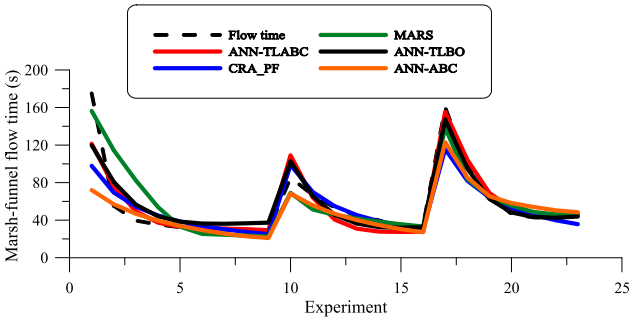


Fig. 14. Comparison of the experimental flow time values with the predicted ones by the CRA-PF, MARS, ANN-ABC, ANN-TLBO, and ANN-TLABC for testing data sets.

5. Conclusion

Irrespective of the cement type, according to Marsh-funnel flow time and mini-slump test results, cement fineness and C_3A content were found to be the most important cement- based parameters affecting the flow performance of the paste mixtures.

Heuristic regression method MARS has the feature of revealing the relative importance of the input variables in the model. According to the model results, the most efficient parameter affecting the paste Marsh-funnel flow time was the admixture content. This was followed by the cement fineness, solid material content of the admixture and cement C_3A content variables. The relative importance of the other input parameters remained very low.

Obtaining the parameters of effective modeling methods with heuristic algorithms has provided a remarkable improvement in prediction studies. The most important feature of heuristic algorithms is that they reach the best solution area in a shorter time by scanning the solution space intuitively. Heuristic algorithms used in this study gave better results than classical methods. The best result in the study was obtained from the ANN-TLABC method in which the ANN coefficients were optimized by using two heuristic algorithms together. Application of heuristic algorithms in predicting the properties of cementitious systems will lead to the improvement of the model accuracy, resulting in significant saving in time and money in the cementitious systems studies.

Table S1
Values of variables used for Marsh-funnel flow time.

Cement type	CF (cm^2/g)	C_3A (%)	C_3S (%)	C_2S (%)	C_4AF (%)	EAC (%)	ASC (%)	Admixture/cement ratio (%)									
								0.5	0.75	1	1.25	1.5	1.75	2	2.25	2.5	2.75
C1	4260	5.85	62.83	13.20	13.63	0.59900	33.5	√*	√	√	√	√	√	√	√	√	–**
C2	3820	2.77	64.03	12.63	15.98	0.60796	33.5	√	√	√	√	√	√	√	√	√	–
C3	3760	1.90	65.73	11.05	16.27	0.50978	33.5	√	√	√	√	√	√	√	√	√	–
C4	3690	–	–	–	–	–	33.5	√	√	√	√	√	√	√	√	√	√
C5	3900	6.92	66.15	11.86	9.68	0.69454	33.5	√	√	√	√	√	√	√	√	√	√
C6	2810	3.58	67.10	10.20	13.13	1.04454	33.5	√	√	√	√	√	√	√	√	–	–
C7	3810	3.15	61.99	13.31	15.23	1.20692	33.5	√	√	√	√	√	√	√	–	–	–
C8	3090	7.92	64.21	11.39	10.27	0.88060	33.5	√	√	√	√	√		–	–	–	–
C9	3510	13.88	52.50	20.37	7.67	1.23220	33.5	√	√	√	√	–	–	–	–	–	–
C1	4260	5.85	62.83	13.20	13.63	0.59900	33.76	√	√	√	√	√	√	√			–
C2	3820	2.77	64.03	12.63	15.98	0.60796	33.76	√	√	√	√	√	√	√	–	–	–
C3	3760	1.90	65.73	11.05	16.27	0.50978	33.76	√	√	√	√	√	√	√	√	√	√
C4	3690	–	–	–	–	–	33.76	√	√	√	√	√	√	√	√	√	√
C5	3900	6.92	66.15	11.86	9.68	0.69454	33.76	√	√	√	√	√	√	√	√	√	√
C6	2810	3.58	67.10	10.20	13.13	1.04454	33.76	√	√	√	√	√	√	√	√	–	–
C7	3810	3.15	61.99	13.31	15.23	1.20692	33.76	√	√	√	√	√	√	√	√	–	–
C8	3090	7.92	64.21	11.39	10.27	0.88060	33.76	√	√	√	√	√	√	–	–	–	–
C9	3510	13.88	52.50	20.37	7.67	1.23220	33.76	√	√	√	√	√	√	–	–	–	–
C1	4260	5.85	62.83	13.20	13.63	0.59900	38.56	√	√	√	√	√	√	√		–	–
C2	3820	2.77	64.03	12.63	15.98	0.60796	38.56	√	√	√	√	√	√	√	–	–	–
C3	3760	1.90	65.73	11.05	16.27	0.50978	38.56	√	√	√	√	√	√	√	√	√	√
C4	3690	–	–	–	–	–	38.56	√	√	√	√	√	√	√	√	√	√
C5	3900	6.92	66.15	11.86	9.68	0.69454	38.56	√	√	√	√	√	√	√	√	√	√
C6	2810	3.58	67.10	10.20	13.13	1.04454	38.56	√	√	√	√	√	√	√	√	√	–
C7	3810	3.15	61.99	13.31	15.23	1.20692	38.56	–	√	√	√	√	√	–	–	–	–
C8	3090	7.92	64.21	11.39	10.27	0.88060	38.56	√	√	√	√	√	–	–	–	–	–
C9	3510	13.88	52.50	20.37	7.67	1.23220	38.56	√	√	√	√	–	–	–	–	–	–

*Experiments with Marsh-funnel flow time value.
**No measurement could be taken due to segregation.

Declaration of Competing Interest

The authors declare that they have no known competing financial interests or personal relationships that could have appeared to influence the work reported in this paper.

Acknowledgements

This study was prepared by using the data obtained from the scope of Assoc. Prof. Dr. Ali Mardani-Aghabaglou's Ph.D. thesis. Assoc. Prof. Dr. Ali Mardani-Aghabaglou took part in the experimental study, the writing and preparation of the paper and the coordination of the team.Prof. Dr. Kambiz Ramyar is Assoc. Prof. Dr. Ali Mardani-Aghabaglou's Ph.D. thesis advisor. He provided support in the preparation and editing of the paper.Assoc. Prof. Dr. Murat Kankal and Assoc. Prof. Dr. Hasan Tahsin Öztürk realized the modeling studies and took part in the writing of the paper.

Appendix

References

[1] D.L. Kantro, Influence of water reducing admixtures on properties of cement paste-a miniature slump test, Cem. Concr. Aggreg. 2 (1980) 95–102.
[2] M. Schatzmann, P. Fischer, G.R. Bezzola, Rheological behavior of fine and large particle suspensions, J. Hydraul. Eng. 129 (2003) 796–803, https://doi.org/10.1061/(ASCE)0733-9429(2003)129:10(796).
[3] M. Schatzmann, G.R. Bezzola, P. Fischer, E.J. Windhab, H.E. Minor, The ball measuring system-a new rheometric tool to determine the flow curve of large particle material, in: Swiss Gr. Rheol. Annu. Meet., Lausanne/Switzerland, 2004.
[4] E. Koehler D. Fowler Development of a Portable rheometer for fresh Portland cement concrete Int. Cent. Aggregates Res. 2004 321 http://www.icar.utexas.edu/publications/105/105-3F.pdf.
[5] A. Tagnit-Hamou, P.C. Aïtcin, Cement and Superplasticizer Compatibility, World Cem. 38–42 (1993).
[6] V.H. Dodson, T.D. Hayden, Another look at the Portland cement/chemical admixture incompatibility problem, Cem. Concr. Aggregates. 11 (1989) 52–56.
[7] D. Bonen, S.L. Sarkar, The superplasticizer adsorption capacity of cement pastes, pore solution composition, and parameters affecting flow loss, Cem. Concr. Res. 25 (1995) 1423–1434, https://doi.org/10.1016/0008-8846(95)00137-2.
[8] S. Erdogdu, Compatibility of superplasticizers with cements different in composition, Cem. Concr. Res. 30 (2000) 767–773, https://doi.org/10.1016/S0008-8846(00)00229-5.
[9] S. Jiang, B.G. Kim, P.C. Aïtcin, Importance of adequate soluble alkali content to ensure cement/superplasticizer compatibility, Cem. Concr. Res. 29 (1999) 71–78, https://doi.org/10.1016/S0008-8846(98)00179-3.
[10] C. Bedard, N.P. Mailvaganam, The use of chemical admixtures in concrete. Part II: Admixture-admixture compatibility and practical problems, J. Perform. Constr. Facil. 19 (2005) 263–266, https://doi.org/10.1061/(ASCE)0887-3828(2005)19:4(263).
[11] S. Hanehara, K. Yamada, Interaction between cement and chemical admixture from the point of cement hydration, absorption behaviour of admixture, and paste rheology, Cem. Concr. Res. 29 (1999) 1159–1165, https://doi.org/10.1016/S0008-8846(99)00004-6.
[12] A. Mardani-Aghabaglou, M. Tuyan, G. Yilmaz, Ö. Ariöz, K. Ramyar, Effect of different types of superplasticizer on fresh, rheological and strength properties of self-consolidating concrete, Constr. Build. Mater. 47 (2013) 1020–1025, https://doi.org/10.1016/j.conbuildmat.2013.05.105.
[13] A. Mardani-Aghabaglou, O.C. Boyaci, H. Hosseinnezhad, B. Felekoğlu, K. Ramyar, Effect of gypsum type on properties of cementitious materials containing high range water reducing admixture, Cem. Concr. Compos. 68 (2016) 15–26, https://doi.org/10.1016/j.cemconcomp.2016.02.007.
[14] A. Mardani-Aghabaglou, B. Felekoğlu, K. Ramyar, Effect of cement C3A content on properties of cementitious systems containing high-range water-reducing admixture, J. Mater. Civ. Eng. 29 (2017), https://doi.org/10.1061/(ASCE)MT.1943-5533.0001925.
[15] A. Mardani-Aghabaglou, A.E. Son, B. Felekoglu, K. Ramyar, Effect of cement fineness on properties of cementitious materials containing high range water reducing admixture, J. Green Build. 12 (2017) 142–167, https://doi.org/10.3992/1552-6100.12.1.142.
[16] P.C. Aïtcin, High Performance Concrete, E&FN Spon, New York, 2004.
[17] A. Oğuz, A Research on Multivariate Adaptive Regression Spline and a Application, Erzincan University, 2014. http://earsiv.ebyu.edu.tr/xmlui/bitstream/handle/20.500.12432/3209/10031557.pdf?sequence=1&isAllowed=y.
[18] V. Chandwani, V. Agrawal, R. Nagar, S. Singh, Modeling slump of ready mix concrete using artificial neural network, Int. J. Technol. 6 (2015) 207–216, https://doi.org/10.14716/ijtech.v6i2.213.
[19] G. Aktas, M.S. Ozerdem, Prediction of behavior of fresh concrete exposed to vibration using artificial neural networks and regression model, Struct. Eng. Mech. 60 (2016) 655–665, https://doi.org/10.12989/sem.2016.60.4.655.
[20] A.R. Ghanizadeh, H. Abbaslou, A.T. Amlashi, P. Alidoust, Modeling of bentonite/sepiolite plastic concrete compressive strength using artificial neural network and support vector machine, Front. Struct. Civ. Eng. 13 (2019) 215–239, https://doi.org/10.1007/s11709-018-0489-z.
[21] E.M. Golafshani, A. Behnood, M. Arashpour, Predicting the compressive strength of normal and High-Performance Concretes using ANN and ANFIS hybridized with Grey Wolf Optimizer, Constr. Build. Mater. 232 (2020), https://doi.org/10.1016/j.conbuildmat.2019.117266 117266.
[22] A. Ashrafian, F. Shokri, M.J. Taheri Amiri, Z.M. Yaseen, M. Rezaie-Balf, Compressive strength of Foamed Cellular Lightweight Concrete simulation: New development of hybrid artificial intelligence model, Constr. Build. Mater. 230 (2020) 117048, https://doi.org/10.1016/j.conbuildmat.2019.117048.
[23] A. Kaveh, T. Bakhshpoori, S.M. Hamze-Ziabari, M5' and mars based prediction models for properties of selfcompacting concrete containing fly ash, Period. Polytech. Civ. Eng. 62 (2018) 281–294, https://doi.org/10.3311/PPci.10799.
[24] A. Gholampour, I. Mansouri, O. Kisi, T. Ozbakkaloglu, Evaluation of mechanical properties of concretes containing coarse recycled concrete aggregates using multivariate adaptive regression splines (MARS), M5 model tree (M5Tree), and least squares support vector regression (LSSVR) models, Neural Comput. Appl. 32 (2020) 295–308, https://doi.org/10.1007/s00521-018-3630-y.
[25] A.H. Aytaç, Effect of Composition of Portland Cement on the Performance of Superplasticizer Admixture, Dokuz Eylül University, 2006.
[26] P.C. Nkinamubanzi, B. Fournier, Evaluation of the Potential Use of the Superplasticizer Alphalith FT30LV with Canadian Cements, 2003.
[27] L. Agulló, B. Toralles-Carbonari, R. Gettu, A. Aguado, Fluidity of cement pastes with mineral admixtures and superplasticizer—A study based on the Marsh cone test, Mater. Struct. 32 (1999) 479–485, https://doi.org/10.1007/BF02481631.
[28] S. Aydın, A. Hilmi Aytaç, K. Ramyar, Effects of fineness of cement on polynaphthalene sulfonate based superplasticizer–cement interaction, Constr. Build. Mater. 23 (2009) 2402–2408, https://doi.org/10.1016/j.conbuildmat.2008.10.004.
[29] S. Jarny, N. Roussel, S. Rodts, F. Bertrand, R. Le Roy, P. Coussot, Rheological behavior of cement pastes from MRI velocimetry, Cem. Concr. Res. 35 (2005) 1873–1881, https://doi.org/10.1016/j.cemconres.2005.03.009.
[30] M. Nehdi, Microfiller Effect on Rheology, Microstructure and Mechanical Properties of High Performance Concrete, University of British Colombia, Canada, 1998.
[31] K. Khayat, A. Yahia, Simple Field Tests to Characterize Fluidity and Washout Resistance of Structural Cement Grout, Cem. Concr. Aggregates. 20 (1998) 145–156. https://doi.org/https://doi.org/10.1520/CCA10448J. ISSN 0149-6123.
[32] A. Shahriar, M.L. Nehdi, Modelling rheological properties of oil well cement slurries using multiple regression analysis and artificial neural networks, J. Mater. Civ. Eng. 3 (2013) 26–37.
[33] H. Eskandari-Naddaf, R. Kazemi, ANN prediction of cement mortar compressive strength, influence of cement strength class, Constr. Build. Mater. 138 (2017) 1–11, https://doi.org/10.1016/j.conbuildmat.2017.01.132.
[34] S. Chithra, S.R.R.S. Kumar, K. Chinnaraju, F. Alfin Ashmita, A comparative study on the compressive strength prediction models for High Performance Concrete containing nano silica and copper slag using regression analysis and Artificial Neural Networks, Constr. Build. Mater. 114 (2016) 528–535, https://doi.org/10.1016/j.conbuildmat.2016.03.214.
[35] T. Nguyen, A. Kashani, T. Ngo, S. Bordas, Deep neural network with high-order neuron for the prediction of foamed concrete strength, Comput. Civ. Infrastruct. Eng. 34 (2019) 316–332, https://doi.org/10.1111/mice.12422.
[36] Ł. Sadowski, M. Nikoo, M. Shariq, E. Joker, S. Czarnecki, The Nature-Inspired Metaheuristic Method for Predicting the Creep Strain of Green Concrete Containing Ground Granulated Blast Furnace Slag, Materials (Basel). 12 (2019), https://doi.org/10.3390/ma12020293.
[37] W.S. Alyhya, S. Kulasegaram, B.L. Karihaloo, Simulation of the flow of self-compacting concrete in the V-funnel by SPH, Cem. Concr. Res. 100 (2017) 47–59, https://doi.org/10.1016/j.cemconres.2017.05.021.
[38] R. Deeb, S. Kulasegaram, B.L. Karihaloo, 3D modelling of the flow of self-compacting concrete with or without steel fibres. Part I: slump flow test, Comput. Part. Mech. 1 (2014) 373–389, https://doi.org/10.1007/s40571-014-0002-y.
[39] F. Badry, S. Kulasegaram, B.L. Karihaloo, Estimation of the yield stress and distribution of large aggregates from slump flow test of self-compacting concrete mixes using smooth particle hydrodynamics simulation, J. Sustain. Cem. Mater. 5 (2014) 117–134, https://doi.org/10.1080/21650373.2014.979266.
[40] M.S. Abo Dhaheer, S. Kulasegaram, B.L. Karihaloo, Simulation of self-compacting concrete flow in the J-ring test using smoothed particle hydrodynamics (SPH), Cem. Concr. Res. 89 (2016) 27–34, https://doi.org/10.1016/j.cemconres.2016.07.016.
[41] R. Deeb, S. Kulasegaram, B.L. Karihaloo, 3D modelling of the flow of self-compacting concrete with or without steel fibres. Part II: L-box test and the

assessment of fibre reorientation during the flow, Comput. Part. Mech. 1 (2014) 391–408, https://doi.org/10.1007/s40571-014-0003-x.
[42] T.E. 934-2+A1, Kimyasal katkılar - Beton, harç ve şerbet için - Bölüm 2: Beton kimyasal katkıları - Tarifler, gerekler, uygunluk, işaretleme ve etiketleme, Türk Standartları Enstitüsü, Ankara, 2002.
[43] D. Kantro, Influence of Water-Reducing Admixtures on Properties of Cement Paste—A Miniature Slump Test, Cem. Concr. Aggregates. 2 (1980) 95–102, https://doi.org/10.1520/CCA10190J.
[44] J.H. Friedman, Multivariate adaptive regression splines (with Discussion), Ann. Stat. 19 (1991) 1–141, https://doi.org/10.1214/aos/1176347969.
[45] W. Zhang, A.T.C. Goh, Multivariate adaptive regression splines and neural network models for prediction of pile drivability, Geosci. Front. (2016), https://doi.org/10.1016/j.gsf.2014.10.003.
[46] S. Suman, Prediction of pile capacity parameters using functional networks and multivariate adaptive regression splines, National Institute of Technology (2015).
[47] S. Khuntia, H. Mujtaba, C. Patra, K. Farooq, N. Sivakugan, B.M. Das, Prediction of compaction parameters of coarse grained soil using multivariate adaptive regression splines (MARS), Int. J. Geotech. Eng. 9 (2015) 79–88, https://doi.org/10.1179/1939787914Y.0000000061.
[48] P. Dey, A.K. Das, Application of multivariate adaptive regression spline-assisted objective function on optimization of heat transfer rate around a cylinder, Nucl. Eng. Technol. 48 (2016) 1315–1320, https://doi.org/10.1016/J.NET.2016.06.011.
[49] D. Karaboga, B. Akay, A comparative study of Artificial Bee Colony algorithm, Appl. Math. Comput. 214 (2009) 108–132, https://doi.org/10.1016/j.amc.2009.03.090.
[50] B. Akay, D. Karaboga, A modified Artificial Bee Colony algorithm for real-parameter optimization, Inf. Sci. (Ny) 192 (2012) 120–142, https://doi.org/10.1016/j.ins.2010.07.015.
[51] R.V. Rao, V. Patel, An improved teaching-learning-based optimization algorithm for solving unconstrained optimization problems, Sci. Iran. 20 (2013) 710–720, https://doi.org/10.1016/j.scient.2012.12.005.
[52] R.V. Rao, V.J. Savsani, J. Balic, Teaching-learning-based optimization algorithm for unconstrained and constrained real-parameter optimization problems, Eng. Optim. 44 (2012) 1447–1462, https://doi.org/10.1080/0305215X.2011.652103.
[53] X. Chen, B. Xu, Teaching-Learning-Based Artificial Bee Colony, in: Y. Tan, S. Y., Tang Q. (Eds.), Adv. Swarm Intell. ICSI 2018., Springer, Cham, 2018: pp. 166–178. https://doi.org/10.1007/978-3-319-93815-8.
[54] D.N. Moriasi, J.G. Arnold, M.W. Van Liew, R.L. Bingner, R.D. Harmel, T.L. Veith, Model Evaluation Guidelines for Systematic Quantification of Accuracy in Watershed Simulations, Trans. ASABE. 50 (2007) 885–900, https://doi.org/10.13031/2013.23153.
[55] W.F. Perenchio, D.L. Kantro, D.A. Whiting, Water Reduction, Slump Loss, and Entrained Air-Void Systems as Influenced by Superplasticizers, ACI Symp. Publ. 62 (1979) 137–156, https://doi.org/10.14359/17723.
[56] W. Prince, M. Edwards-Lajnef, P.C. Aïtcin, Interaction between ettringite and a polynaphthalene sulfonate superplasticizer in a cementitious paste, Cem. Concr. Res. 32 (2002) 79–85, https://doi.org/10.1016/S0008-8846(01)00632-9.